Inversion of Magnetotelluric (MT) Data with Enhanced Structural Fidelity*

Federico Golfré Andreasi[1], Simone Re[1], Federico Ceci[1], and Luca Masnaghetti[1]

Search and Discovery Article #42333 (2018)**
Posted December 24, 2018

*Adapted from extended abstract based on oral presentation given at 2018 International Conference and Exhibition, Cape Town, South Africa, November 4-7, 2018
 DOI:10.1306/42333Andreasi2018

[1]Schlumberger, Milan, Italy (fandreasi@slb.com)

Abstract

Oil and gas exploration in foothill areas is challenged by several factors. The accessibility is not straightforward due to steep terrains and, in some cases, also due to forest coverage; thus, making both exploration and development plans far more expensive. A comprehensive understanding of the subsurface is of paramount importance to target the most promising prospects and to reduce the footprint – and the cost – of exploration and production activities.

Satellite imagery and airborne acquisition techniques can be used to cover large areas in an economic manner and to gain a preliminary knowledge of the subsurface. Unfortunately, these techniques lack the resolution required to infer the geologic setting at depth and to build a structural model with adequate confidence; this is the time when it becomes necessary to step into ground exploration. Seismic imaging techniques are the main tools used to build an accurate description of the subsurface; however, in thrust-belt areas, the signal-to-noise ratio of the seismic reflections is severely reduced by the steep topography and by the almost vertical layering of the formations.

The Magnetotelluric (MT) method has been successfully used as a complementary tool in the exploration of foothill plays (Tartaras et al., 2011): the resistivity sections obtained from the inversion of MT data can be used to derive information about the shape of the subsurface structures and to delineate the boundaries between geological units based on resistivity changes (Deng and Yin, 2016). However, the intrinsic non-uniqueness of the MT inversion process and its lack of structural fidelity could limit the amount of useful information that can be retrieved from the methodology and that can then be exploited by the interpreter. Since the solution of a non-unique inverse problem is heavily dependent on its starting point, a traditional method to tackle the non-uniqueness relies on the careful definition of the starting model, used as a tool for injecting the available apriori information into the inverse problem (Zerilli et al., 2012).

In this work, we present an alternative approach to the exploitation of the apriori knowledge that, instead of embedding it into the starting model, relies on the continuous assimilation of the structural and geological information into the resistivity volume. The method we propose for the inversion of the MT soundings tries to maximize, simultaneously, the data-fit and the structural fidelity: the structural fidelity is defined in

least-square sense as the similarity of the current resistivity model and of the "guiding model" which expresses and synthesizes the apriori knowledge in terms of shape and geometry of the structures. We discuss the advantages and the possible drawbacks deriving from the application of this technique by mean of a synthetic example representative of a foothills play.

The Synthetic Model

The 1994 Amoco statics test dataset was created at the Amoco Tulsa Research Lab in 1994 by Mike O'Brien as part of a project to study methods for attacking static corrections in land data. The geology of the model is completely invented, not based on any specific play, and contains many different types of near-surface geology, generally representing geology thought to be responsible for statics. Even though the model was explicitly designed for static correction issues, it has the very challenging structural features typical of the thrust-belt areas where seismic imaging struggles due to the heterogeneity of the near surface but also due to the complex geometry of the reflectors that have been bent by the compressive tectonics. For these reasons, this dataset is an ideal candidate for studying and analyzing a geologically-driven approach for the inversion of magnetotelluric data and to see how this approach can be used to complement the seismic imaging.

In order to perform the study, we took the velocity model that was used to generate the seismic traces (Figure 1a) and we mapped the velocity into the resistivity using the values reported in Table 1. Figure 1b shows the resistivity model obtained from the conversion process and, for each of the five zones highlighted, we can clearly identify a peculiar feature that the imaging based on the inversion of the magnetotelluric data should recover:

I. The relatively shallow conductive layering.
II. The highly resistive outcropping anomaly and the thin thrust.
III. The shape of the thrust and the conductive feature below the thrust.
IV. The thrust split with the resistive-conductive-resistive sequence.
V. The outcropping portion of the thrust and the massive resistive block on the edge of the model.

The model has an extent of 50 km with a topography excursion of 1200 m going from 300 m above sea level (a.s.l.) in the plain portion up to 1500 m a.s.l.; the maximum depth of the model is 4.5 km. We simulated a magnetotelluric survey by means of 3D finite difference code with a station spacing of 500 m and the acquisition of MT soundings over a frequency range varying from 0.01 Hz to 10 kHz with 11 samples per frequency decade.

The Inversion Method

We solve the inverse MT problem by minimizing a cost function through a preconditioned non-linear conjugate gradient technique, as described by Golfré Andreasi and Masnaghetti (2015). The cost function to be minimized by the inversion process can be written as:

$$\Phi(\mathbf{m}) = \Phi_D(\mathbf{m}) + \Phi_R(\mathbf{m})$$

where $\Phi_D(\mathbf{m})$ represents the data misfit term as a function of the model parameter vector to be inferred ($\mathbf{m}$) and $\Phi_R(\mathbf{m})$ is a regularization term that imposes some smoothness constraint over the spatial distribution of the model parameters. Expanding the Φ_D term and the Φ_R term we have:

$$\Phi_{\mathrm{D}}(\mathbf{m}) = |F(\mathbf{m}) - d_o|^T \mathbf{C}_{\mathrm{D}}^{-1} |F(\mathbf{m}) - d_o|$$

$$\Phi_{\mathrm{R}}(\mathbf{m}) = \tau |\mathbf{m} - \mathbf{m}_{pri}|^T \mathbf{L}^T \mathbf{L} |\mathbf{m} - \mathbf{m}_{pri}|$$

In the equation of the data misfit term, F is the forward modelling operator, d_o represents the observed data and $\mathbf{C}_{\mathrm{D}}^{-1}$ is the inverse of the data covariance matrix. In the equation expressing the regularization term, $\mathbf{m}_{pri}$ is the a priori model, $\mathbf{L}^T\mathbf{L}$ is the regularization operator and the scalar τ is a trade-off parameter that controls the amount of regularization that goes into the inverse problem. In this formulation, the a priori information is inserted into $\mathbf{m}_{pri}$. In fact, the inverse process will try to minimize the data misfit by moving away from the a priori model and this tendency will be counterbalanced by the regularization term that will penalize any variation from the a priori model causing an increase of the cost function.

This approach has two main drawbacks: on one side, the choice of the a priori model is heavily biasing the outcome of the inversion of ill-posed problems such as inversion of MT data. On the other side, this approach fixes the knowledge in the a priori model and requests the inversion to move smoothly away from it.

To overcome these limitations, we can change the inverse problem formulation by decoupling the a priori information source from the a priori model choice. The goal is to inject the available knowledge on the geological setting into the inverse process without acting on the a priori model. This can be achieved by modifying the cost function in the following manner:

$$\Phi(\mathbf{m}) = \Phi_D(\mathbf{m}) + \Phi_R(\mathbf{m}) + \lambda \Phi_G(\mathbf{m})$$

where $\Phi_G(\mathbf{m})$ is the term that constrains – in a least-square sense – the spatial distribution of the resistivity to follow some predefined geometry. With the problem formulated in this way, the inversion algorithm tries to find a solution that satisfies the data $\Phi_{\mathrm{D}}(\mathbf{m})$, the generic spatial smoothness constraint $\Phi_R(\mathbf{m})$ and the structural or geological constraint $\Phi_G(\mathbf{m})$. The scalar parameter λ controls the degree of structural fidelity that the inversion must follow; higher values of λ lead to a resistivity model that favors the similarity with the a priori structural information at the expense of the data fit.

The $\Phi_{\mathrm{G}}(\mathbf{m})$ term is built using an image that defines the shape of the subsurface structures. Among the various possibilities, that image can be derived from an existing map of the geological units or from an interpretation of a vintage seismic section. For instance, the reference image that we defined for our synthetic tests is defined in Figure 2 and it is composed by three different regions. We propose two different methods for building the structural regularization term $\Phi_{\mathrm{G}}(\mathbf{m})$.

The first one is based on the definition of an empirical function f that goes from the discrete domain of the regions into the continuous domain of the resistivity thus defining a "reference" resistivity model. The minimum of this term of the cost function is "located" in correspondence of a resistivity model that is equal to the reference one. If we indicate with $\Phi_{GE}(\mathbf{m})$ this geology-driven regularization term, it can be expressed as:

$$\Phi_{GE}(\mathbf{m}) = \lambda|\mathbf{m} - f(\mathbf{k})|^2; \quad f: \mathbb{N} \rightarrow \mathbb{R},$$

where f is the function mentioned above, **k** represents the spatial distribution and variation of guiding model and $|\cdot|^2$ indicates the L2-norm of the quantity in the brackets. The pre-requisite for the adoption of this regularization scheme is some degree of apriori knowledge about the value of the resistivity distribution within each of the regions defined by the guiding image.

The second method does not require any knowledge or any hypothesis about the resistivity distribution and relies on the geometrical similarity between the resistivity model and the guiding image in order to shape a resistivity model that satisfies also the structural constraint. The degree of structural similarity is quantified by the cross-gradient of the resistivity model with the reference **r** (De Stefano et al., 2011; Gallardo and Meju, 2007); the corresponding $\Phi_{GX}(\mathbf{m})$ regularization term can be expressed as:

$$\Phi_{GX}(\mathbf{m}) = \lambda|\nabla\mathbf{m} \times \nabla\mathbf{r}|^2$$

Zero values of the cross-gradient function correspond to points where spatial changes in both the resistivity distribution **m** and the reference model **r** align. However, the function is also zero where the magnitude of the spatial variations of **m** and/or **r** is negligible, for instance where one or both of them are very smooth or constant.

Inversion Results

We tested the two different techniques presented for injecting the geological apriori information into the MT inversion on the synthetic dataset that we derived from the 1994 Amoco statics test dataset.

The inversion results obtained with the method making use of the empirical function are shown in Figure 3, where, for convenience, we report also the starting model and the true model. In this case the inversion started from a uniform half-space and converged after 25 iterations. Since we are providing a reference image that is substantially correct from a structural standpoint, the inversion result contains all the traits that are present in the synthetic model. In the data space, we can evaluate the inversion results in terms of root-mean-square error (RMSE) that we define as the ratio between the square root of the data misfit term, $\Phi_D(\mathbf{m})$, divided by the number of data points, N. In formulas:

$$\mathrm{RMSE} = \sqrt{\frac{\Phi_D(\mathbf{m})}{N}}$$

The initial RMSE value is equal to 13.47, while the final is 2.26, slightly bigger than the final RMSE of the unconstrained inversion equal to 2.24.

The results of the inversion obtained with the approach based on the cross-gradients are, instead, shown in Figure 4. In this case the inversion could not start from the uniform half-space in order to avoid having an initial cross-gradient contribution identically null. Thus, as a starting point for the inversion, we selected an intermediate model from the unconstrained inversion workflow. The inversion algorithm converged after 14 iterations (21 if we consider also the one needed to get a suitable starting model) with a final RMSE of 2.55.

The resistivity sections obtained with the geologically-driven approach, regardless if empirical or cross-gradients, show interesting features that are not recovered by the unconstrained workflow. For instance, looking at the zone IV, we can appreciate that there is a split of the two thrusting features while the unconstrained inversion was able to recover only a unique resistive feature. Also, the slopes and the shapes of the resistive features in zones II and III are better recovered by the geologically driven approaches. Finally, in zone I, the workflow based on the cross-gradients is recovering quite nicely the conductive feature which, instead, is a bit blurred in the resistivity section obtained with the empirical function.

In the MT inversion workflow, the capability of reconstructing the sharp boundaries delineating the structures in the subsurface with a high degree of fidelity is limited by the "integral effect" of the apparent resistivity and by the generic regularization term $\Phi_R(\mathbf{m})$ that privileges the smoothness of the solution. While the "integral effect" factor is intrinsic of the methodology cannot be compensated, we can easily act on the construction of the cost function and add a term that is favouring the sharpest among the smooth solutions that are satisfying the data to a certain acceptable degree.

One interesting way to compare the inversion results from a data-fit perspective is to look at the RMSE site by site and to display it as a map or, for a 2D case like the one we are examining, as a curve along a profile. The RMSE profiles for the three different inversion results are shown in Figure 5. It is interesting to notice that, on average, final RMSE levels corresponding to the three different results are very similar in zones II and III, however the final resistivity sections in that portion show some quite remarkable differences. This highlights the non-unique nature of the inverse problem in exam and how it is possible to restrict the pool of solutions fitting the data to the ones that have more relevance with respect to some apriori knowledge.

Instead, from a model-space perspective it is interesting and useful to evaluate the "focusing effect" of the geological regularization. With the term "focusing effect" we indicate the capability of the structural regularization to obtain a uniform value of the resistivity within a uniform region of the reference image. This effect can be easily evaluated by looking at the statistical distribution of the resistivity values within each of the regions identified by the guiding image. A strong focusing effect corresponds to a spiky histogram with all the resistivity values concentrated in a narrow resistivity range; on the other hand, a poor focusing effect leads to a flatter histogram with values spread over a wider resistivity range. Figure 6 shows the histogram for each of the three regions depicted in Figure 2 and for the three different inversion results. It is not surprising that the solution with the greatest focusing effect is the one based on the empirical function (blue line) because this option

requires some hypothesis on the resistivity value within each of the regions in order to be able to build the function f and the minimization of the $\Phi_G(\mathbf{m})$ term favors the resistivity value defined used to build that function.

Throughout the lifetime of an exploration project, different versions of interpretations could be provided by the team of geologists, who continuously update their conceptual models based on the available geophysical and drilling results. At the beginning of the project we would tend to have a limited amount of available apriori information with limited reliability. As the project progresses, fresh data become available allowing to refine and to consolidate the knowledge of the prospect. In such a dynamic context it is of paramount importance the possibility to balance the relevance that the reference model has on the outcome of the inversion. As already mentioned, in the approach proposed, the impact of the apriori information on the inversion results is controlled by the scalar value λ that multiplies the geological regularization term $\Phi_G(\mathbf{m})$.

To simulate the context of a real project and to test the effect of the scaling parameter λ, we repeated the inversion exercise with the cross-gradients approach using a "wrong" guiding image – shown in Figure 7a – and changing the weight of the geological constraint. The results of the exercise are reported in Figure 7. Going from Figure 7b to Figure 7d the value of the parameter λ decreases from 10 down to 0.1: basically, we are going from a situation where the geological constraint is over-weighted to a scenario where it is down-weighted passing through an equally-weighted case. Looking at the over-weighting scenario, we can appreciate how the lack of sensitivity of the data to certain resistive features allowed the inversion to progress totally driven by the geologic regularization term. On the other hand, the down-weighted case tends to be very similar to the unconstrained result shown in Figure 1c. It is interesting to see the effect of the reference model in zone II and how the inversion works on removing the resistive feature as soon as the weighting scheme allows the data driven part to prevail (i.e. equally weighted and down-weighted scenarios).

The final RMSE values reached by the three inversion scenarios are 3.0 for the over-weighted case, 2.75 for the equally-weighted case and 2.69 for the down-weighted one. The increase in the RMSE when going from the under-weighting to the over-weighting of the structural constraint indicates that the inversion process is being steered towards a solution less capable of satisfying the data. The posterior analysis of the data misfit and of the model updates must always be considered in the workflow to assess the inversion results. The generation of data residuals (i.e. synthetic versus observed data), including variances and the noise model applied during the inversion, should be carefully analyzed to evaluate the reliability of the inverted resistivity model.

Conclusions

We presented a technique for inverting MT data that embeds in the inverse problem formulation the available apriori geological information. We proposed two possible implementations of the techniques, one based on the use of an empirical function that maps the structural information into a resistivity value and another one that is based on the cross-gradients and brings the structural information in the resistivity model by imposing a geometrical similarity constraint. The approach presented is effective for inferring further geological insight from the available MT data when new information become available, for example in areas surrounding some already exploited resources or after new drilling results.

We demonstrated on a deliberately created synthetic dataset, from an industry recognized geological benchmark, the effectiveness of the technique in enhancing the structural fidelity of magnetotelluric data inversion with respect to the unconstrained approach. We compared the results of the two different implementations of the technique, analyzing their strengths and their weaknesses.

We also highlighted the risks associated with a blind application of the technique and how the intrinsic non-uniqueness of the MT inversion could lead to a wrong resistivity model despite a good data fit. This risk can be mitigated by a thorough exploration of the model space along with a careful examination of the misfit residuals to understand which features of the model are reliable and which are potentially enforced by the structural constraint (Constable et al., 2015).

Acknowledgements

The authors acknowledge Amoco and BP that kindly provided the 1994 Amoco statics test dataset (aka 1994 BP statics benchmark model) that was created by Mike O'Brien and Carl Regone in 1994.

References Cited

Constable, S., A. Orange, and K. Key, 2015, And the geophysicist replied: "Which model do you want?": Geophysics, v. 80/3, E197-E212.

De Stefano, M., F. Golfré Andreasi, S. Re, M. Virgilio, and F.F. Snyder, 2011, Multiple-domain, simultaneous joint inversion of geophysical data with application to subsalt imaging: Geophysics, v. 76/3, R69-R80.

Gallardo, L.A., and M.A. Meju, 2007, Joint two-dimensional cross-gradient imaging of magnetotelluric and seismic traveltime data for structural and lithological classification: Geophysical Journal International, v. 169/3, p. 1261-1272.

Golfré Andreasi, F., and L. Masnaghetti, 2015, Decoupled Model Grids for Simultaneous Joint Inversion of MT and CSEM Data: 77th EAGE Conference and Exhibition Extended Abstracts, N105.

Hui, C., J. Deng, and C. Yin, 2016, Three-dimensional electrical structures of Jiurui ore district in the middle-lower Yangtze River Metallogenic Belt, eastern China from AMT inversion: 86th SEG International Exposition and Annual Meeting, Extended Abstracts.

Tartaras, E., L. Masnaghetti, A. Lovatini, S. Hallinan, M. Mantovani, M. Virgilio, W. Soyer, M. De Stefano, F. Snyder, J. Subia, and T. Dugoujard, 2011, Multi-property earth model building through data integration for improved subsurface imaging: First Break, v. 29/4, p. 83-88.

Zerilli, A., A. Lovatini, A. Battaglini, and P.D.L. Menezes, 2012, Resolving Complex Overthrust Features Using Magnetotellurics – The Bolivian Foothills Case Study: First EAGE/ACGGP Latin American Geophysics Workshop.

Velocity [m/s]	Resistivity [Ωm]
[600, 2000)	4
[2000,3000)	8
[3000,4000)	30
[4000,4700)	100
≥4700	800

Table 1. Values used for converting the velocity into the resistivity.

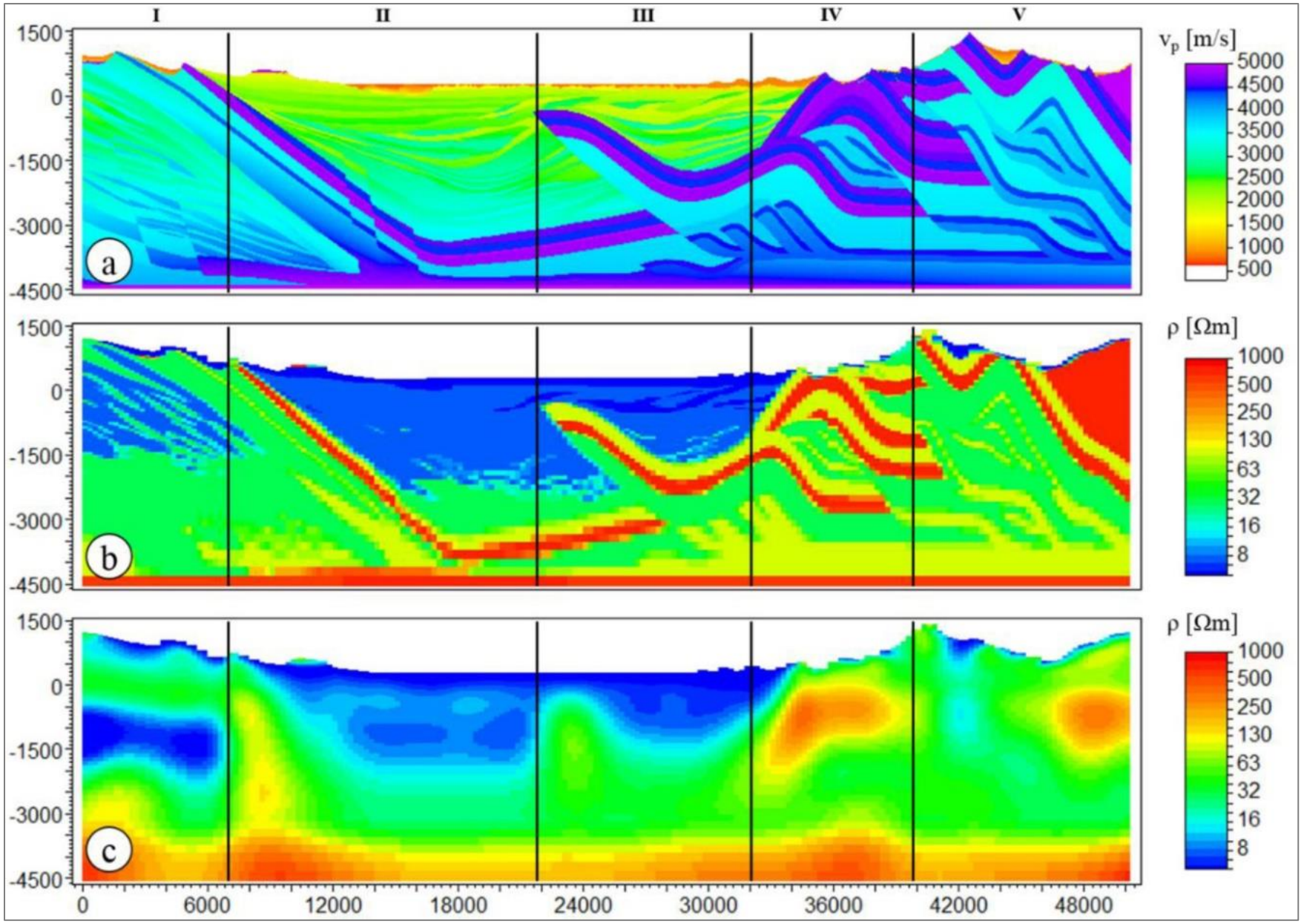

Figure 1. (a) Velocity model. (b) Resistivity model obtained through conversion of the velocity model with the various zones highlighted. (c)Resistivity model from inversion without geological constraint.

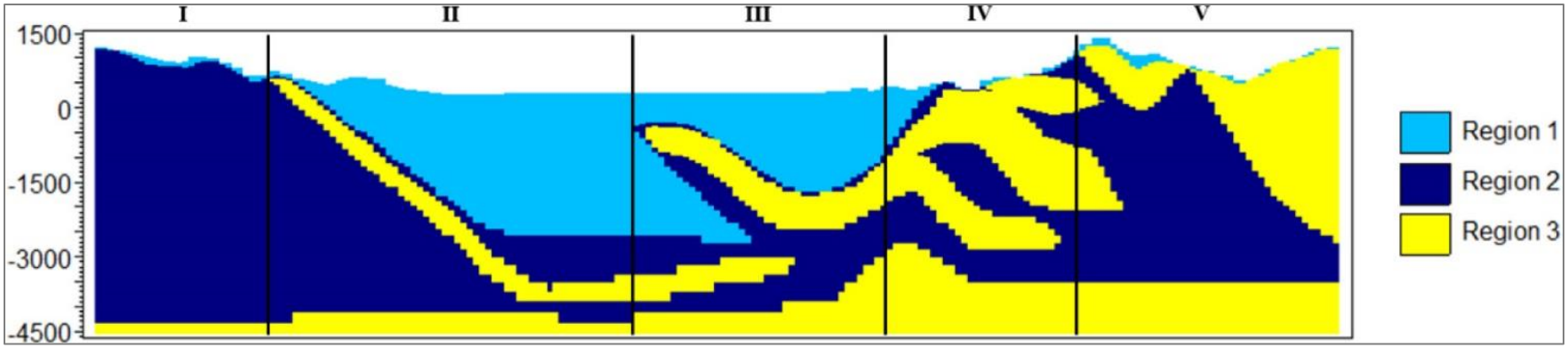

Figure 2. Reference image used to build the structural regularization terms.

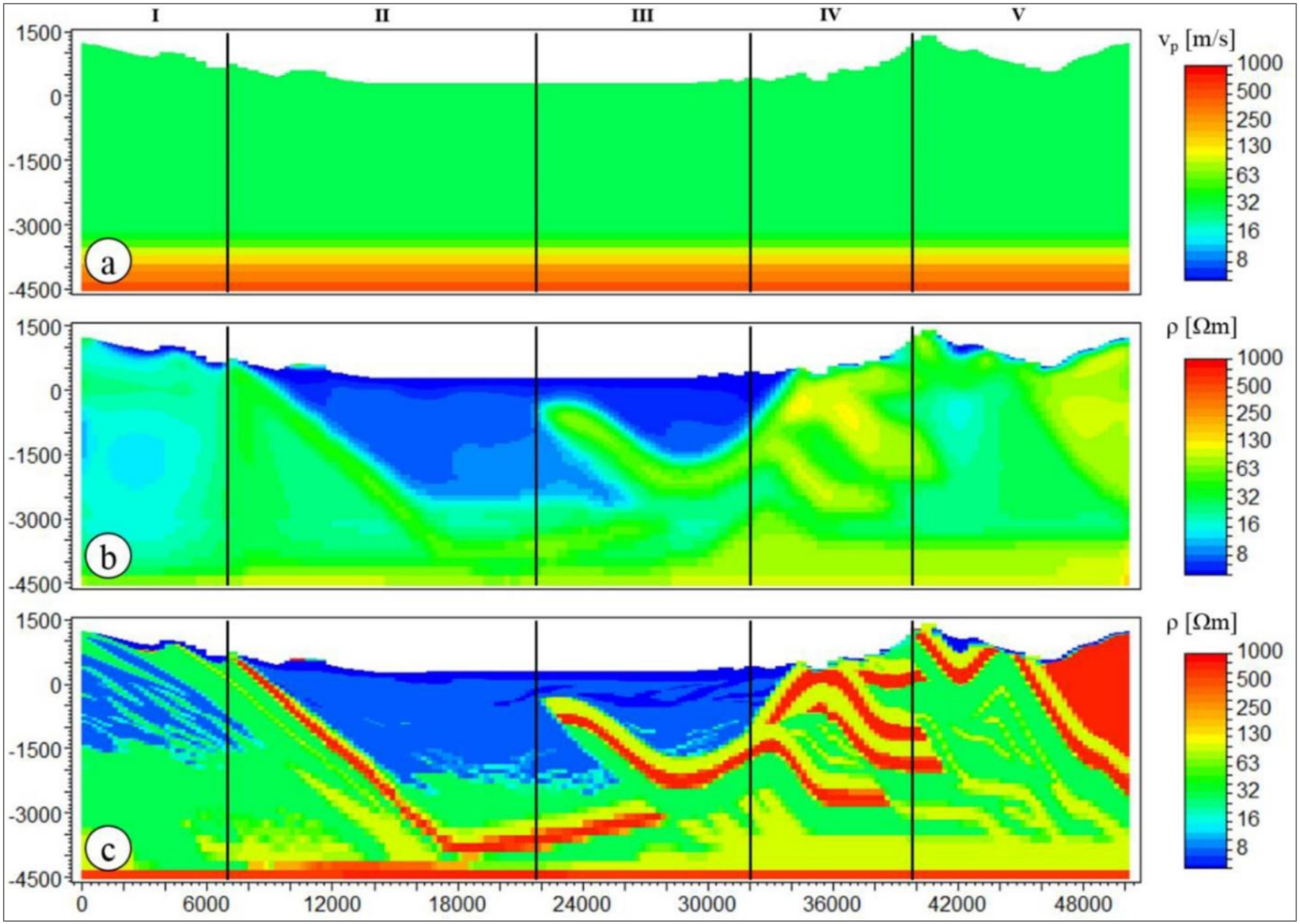

Figure 3. Inversion workflow making use of the "empirical" constraint. (a) Starting model, (b) inverted model after 25 iterations, and (c) true resistivity model.

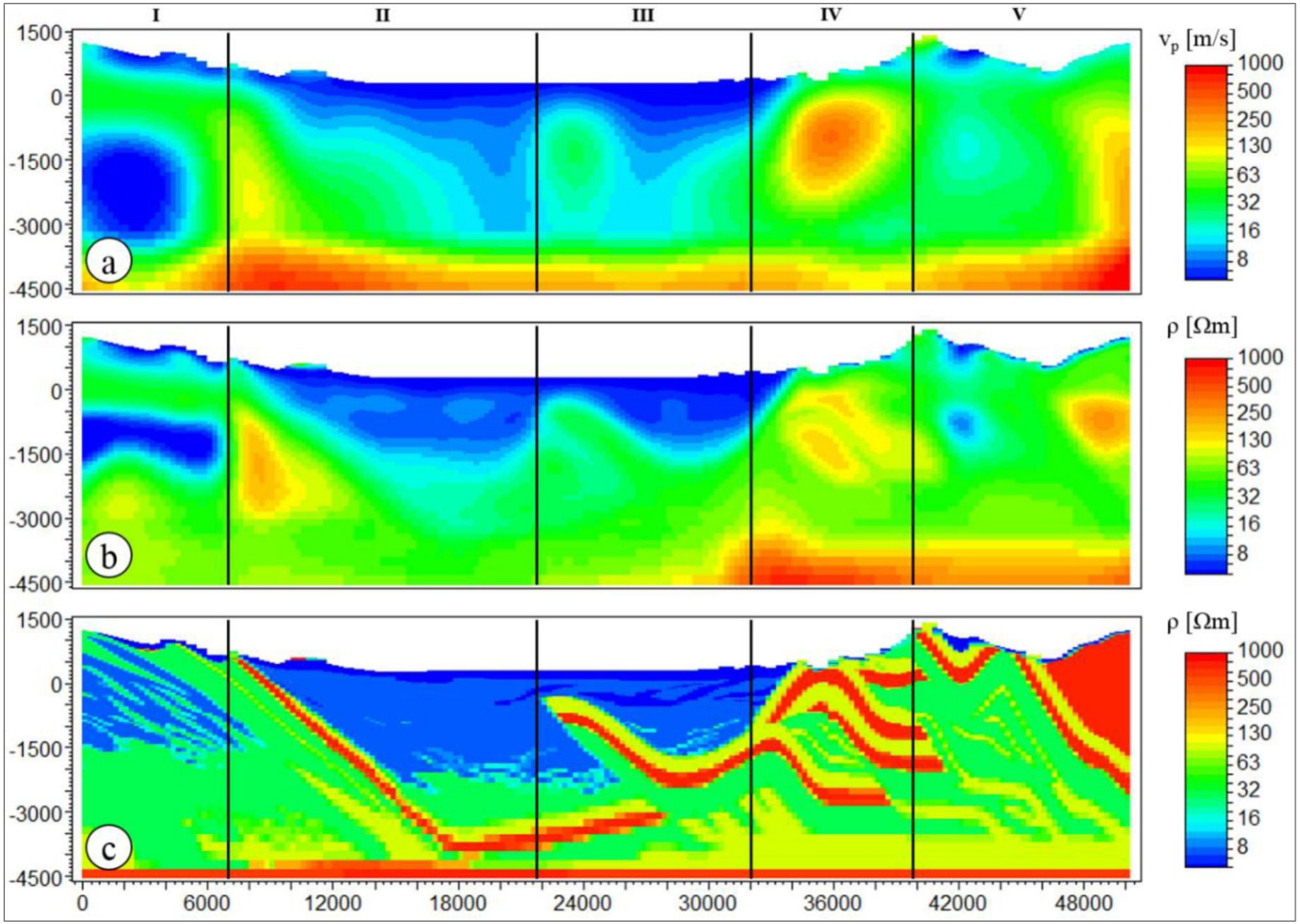

Figure 4. Inversion workflow making use of the cross-gradient constraint. (a) Starting model, (b) inverted model after 14 iterations, and (c) true resistivity model.

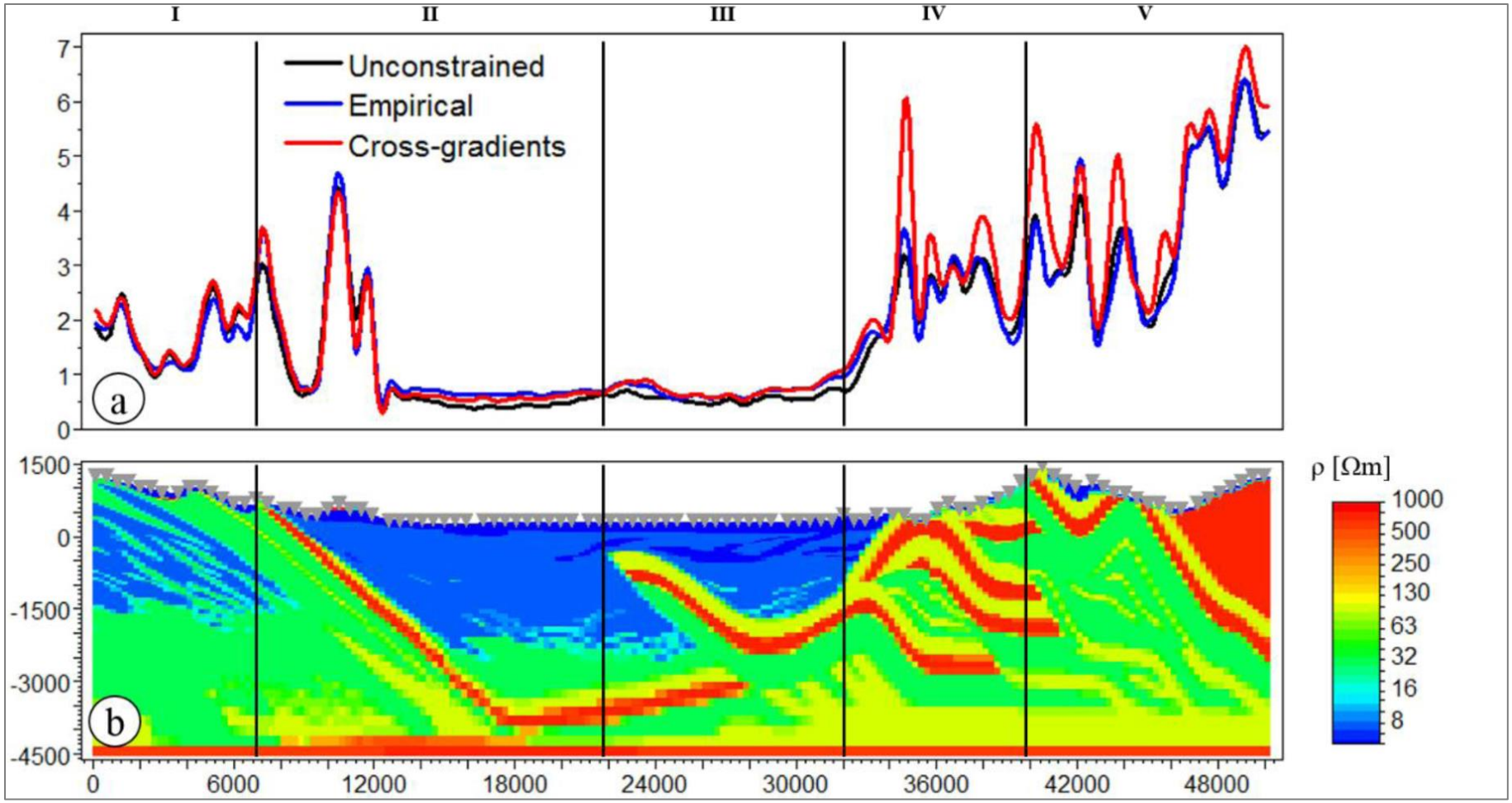

Figure 5. (a) The RMSE profile for the three different inversion scenarios: unconstrained (black line), with empirical constraint (blue line) and with cross-gradients constraint (red line). (b) The true resistivity model.

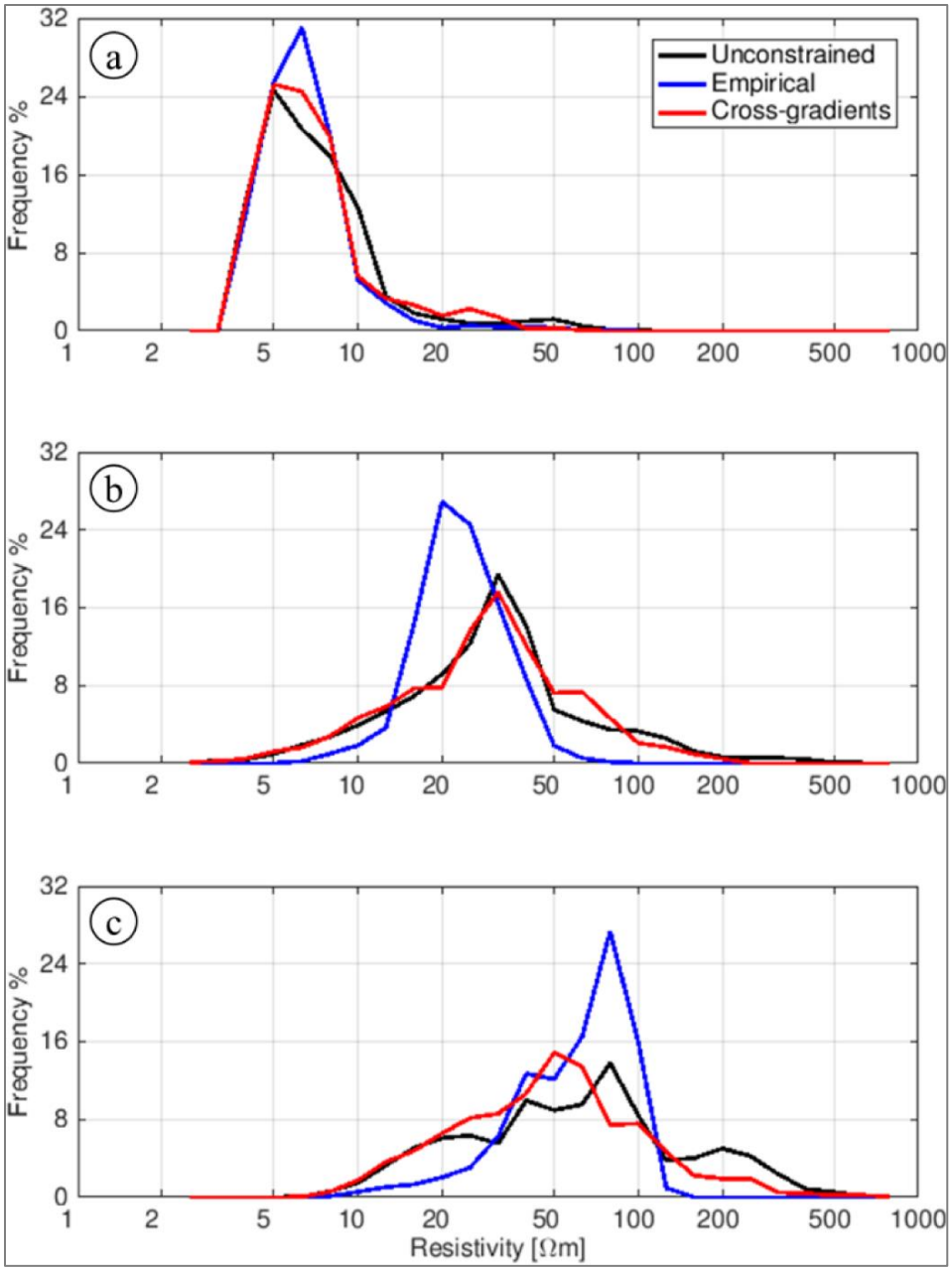

Figure 6. Histograms of the resistivity values obtained by the inversion within each of the regions defined in Figure 2. From top to bottom, (a) region 1, (b) region 2, and (c) region 3. The three different results are instead color-coded: black for the unconstrained inversion, blue for the solution based on the empirical function and red for the result obtained with the cross-gradients approach.

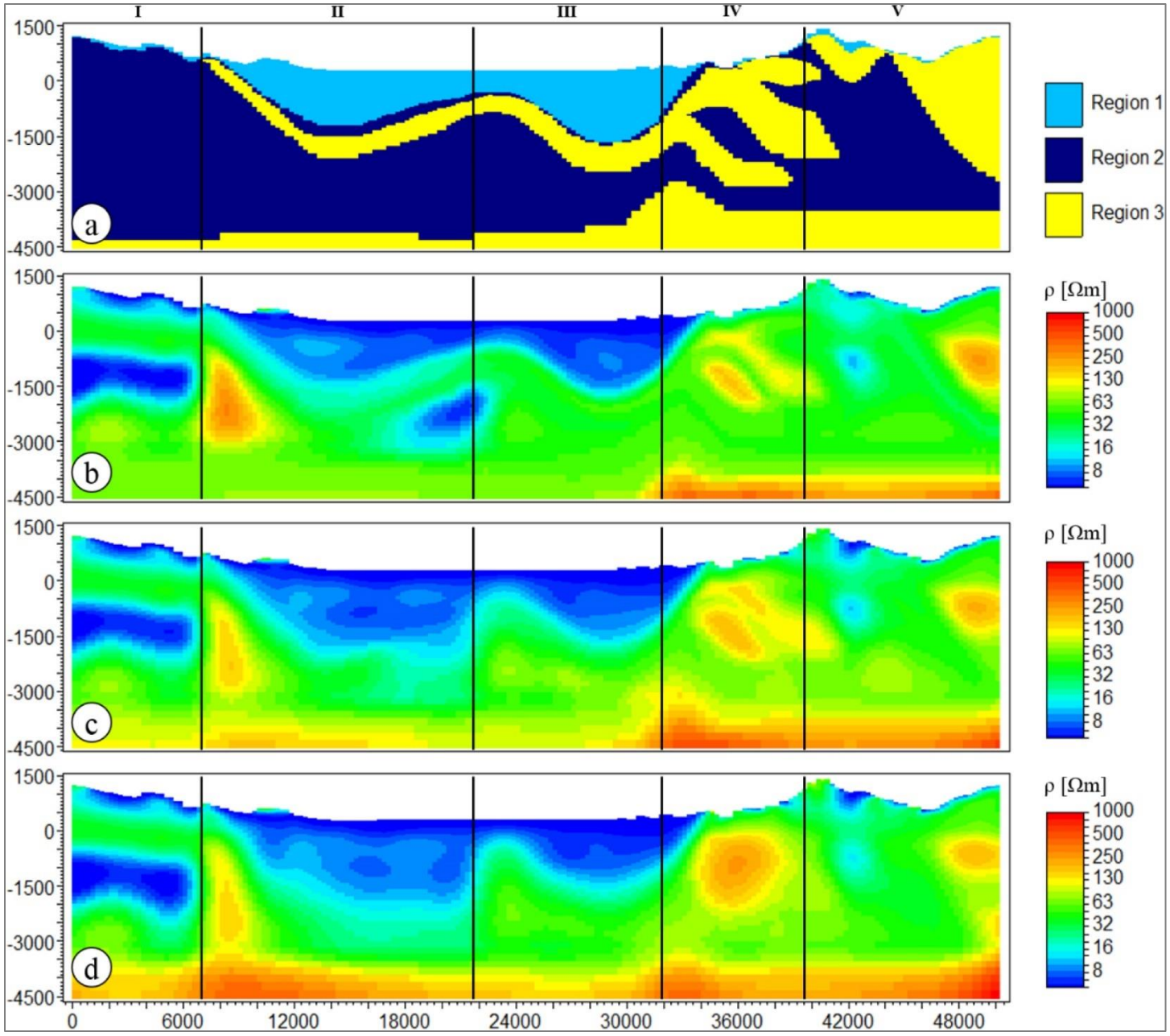

Figure 7. (a) The "wrong" guiding image is used to test the effect of the structural constraint weight on the inversion result. (b) The constraint is over-weighted (i.e. $\lambda = 10$), in (c) it is equally weighted (i.e. $\lambda = 1$) and, finally, in (d) it is down-weighted (i.e. $\lambda = 0.1$).